THE JOURNAL OF BIOLOGICAL CHEMISTRY VOL. 291, NO. 42, pp. 21869–21879, October 14, 2016

Glucose-independent Acetate Metabolism Promotes Melanoma Cell Survival and Tumor Growth*[S]

Received for publication, April 21, 2016, and in revised form, August 15, 2016 Published, JBC Papers in Press, August 18, 2016, DOI 10.1074/jbc.M115.712166

Alexander J. Lakhter[‡], James Hamilton[§], Raymond L. Konger[¶], Nickolay Brustovetsky[§], Hal E. Broxmeyer[‡], and Samisubbu R. Naidu[‡1]

From the [‡]Department of Immunology and Microbiology, Indiana University School of Medicine, Indianapolis, Indiana 46202, [§]Department of Pharmacology and Toxicology, Indiana University School of Medicine, Indianapolis, Indiana 46202, and [¶]Department of Pathology, Indiana University School of Medicine, Indianapolis, Indiana 46202

Tumors rely on multiple nutrients to meet cellular bioenergetics and macromolecular synthesis demands of rapidly dividing cells. Although the role of glucose and glutamine in cancer metabolism is well understood, the relative contribution of acetate metabolism remains to be clarified. We show that glutamine supplementation is not sufficient to prevent loss of cell viability in a subset of glucose-deprived melanoma cells, but synergizes with acetate to support cell survival. Glucose-deprived melanoma cells depend on both oxidative phosphorylation and acetate metabolism for cell survival. Acetate supplementation significantly contributed to maintenance of ATP levels in glucose-starved cells. Unlike acetate, short chain fatty acids such as butyrate and propionate failed to prevent loss of cell viability from glucose deprivation. *In vivo* studies revealed that in addition to nucleo-cytoplasmic acetate assimilating enzyme ACSS2, mitochondrial ACSS1 was critical for melanoma tumor growth in mice. Our data indicate that acetate metabolism may be a potential therapeutic target for BRAF mutant melanoma.

Malignant cells undergo metabolic reprograming to fuel proliferation in a nutrient-limited environment. Tumor cells metabolize glucose in the presence of oxygen, a process known as the Warburg effect or aerobic glycolysis (1). The Warburg effect is generally considered as a metabolic hallmark of cancer (2), yet therapeutic targeting of underlying pathways has remained challenging. For example, BRAF inhibitors are the first line therapy for treatment of patients with mutant BRAF-driven melanoma (3). However, rapid development of resistance to these inhibitors involves reduction in glucose uptake and glycolysis (4, 5). Recent studies demonstrated that tumor cells are dependent on glutamine metabolism to support cell proliferation (6). Glutamine metabolism enables maintenance of tricarboxylic acid (TCA)[2] cycle intermediates and plays a critical role in suppressing oxidative stress by supplying antioxidants. Although glutamine can synergize with glucose metabolism to support tumor cell proliferation, metabolic tracing studies in glucose-deprived cells revealed that an unknown source of carbon cooperated with glutamine in maintaining TCA cycle intermediates (7). Collectively, these studies suggest that malignant cells rapidly adapt to nutrient limitation by resetting their metabolism to maintain cell proliferation, thus hampering effective treatments.

Similar to DNA synthesis, energy production and lipid synthesis are crucial biochemical processes in rapidly dividing cancer cells. Acetyl-CoA, a mitochondrial metabolite responsible for the TCA cycle and energy production is also the primary substrate for lipid synthesis. ATP citrate lyase (ACLY) plays a central role in mobilizing acetyl-CoA from the mitochondria to the cytoplasm. ACLY overexpression is frequently observed in tumors and its inhibition reduces tumor growth (8). Although BRAF inhibitor resistant melanoma shows reduced glucose uptake (4, 5), as opposed to the Warburg effect, these tumors gain mitochondrial functions to retain malignant growth potential (9–12). Moreover, the Warburg effect limits the entry of carbon into mitochondria by promoting lactate production (13). We reasoned that in addition to glutamine metabolism there must be other sources of carbon that contribute to acetyl-CoA production to support the growth of melanoma cells.

Clinical imaging studies using [^{11}C]acetate have established rapid uptake of acetate in several solid tumors (14–16). Importantly, tumors that showed reduced glucose uptake correlated with enhanced acetate uptake (17). These clinical studies led to a renewed interest in acetate metabolism. Acetyl-CoA synthetases (ACSS) catalyze conversion of acetate to acetyl-CoA in an ATP-dependent reaction. Two major ACSS enzymes account for acetate metabolism in cells. ACSS1 (also known as Acecs2) is localized to the mitochondria, whereas ACSS2 (also known as Acecs1) functions both in the cytoplasm and the nucleus (18, 19). A recent study showed that ACSS2 is responsible for the majority of the acetate uptake, and demonstrated a reduced tumor burden in an ACSS2 mutant hepatocellular carcinoma mouse model (20). ACSS2-mediated acetate metabolism con-

* This work was supported in part by the Indiana CTSI Independent Scientist Award, Indiana CTSI Core awards, and the Showalter award (to S. R. N.) and National Institutes of Health Grant NS078008 (to N. B.). Hal Broxmeyer committed significant financial resources for completion of this project. The authors declare that they have no conflicts of interest with the content of this article. The content is solely the responsibility of the authors and does not necessarily represent the official views of the National Institutes of Health.

[S] This article contains supplemental Figs. S1–S6.

[1] To whom correspondence should be addressed: Dept. of Immunology and Microbiology, Indiana University School of Medicine, Indianapolis, IN 46202. Tel.: 317-278-5086; E-mail: naidus@iu.edu.

[2] The abbreviations used are: TCA, tricarboxylic acid; ACLY, ATP citrate lyase; ACSS, acetyl-CoA synthetase; GTA, glyceryl triacetate; GTP, glyceryl tripropionate; GTB, glyceryl tributyrate; OCR, oxygen consumption rate; ECAR, extracellular acidification rate.

tributes to lipid synthesis and aggressive growth in glioblastoma and breast cancer (21, 22). Although ACSS1 knockdown cells showed reduced acetate uptake and cell growth similar to ACSS2 knockdown (17), the role of ACSS1 is not well understood. Here we show that glucose-starved melanoma cells are highly dependent on acetate to sustain ATP levels, cell viability and proliferation. Conversely, depletion of ACSS1 or ACSS2 reduced melanoma tumor growth in mice. Collectively, our data demonstrate acetate metabolism as a liability in melanoma.

Experimental Procedures

Cell Culture—A375, MEL 526, and MEL697 melanoma cell lines were maintained in RPMI 1640 medium containing 0.3 g/liter L-glutamine (HyClone), 2 g/liter D-glucose (HyClone), and 10% FBS (Sigma) and penicillin/streptomycin (Life Technologies). Cells were routinely tested for mycoplasma contamination with QuickTest Mycoplasma Detection Kit (Biotool).

Antibodies and Reagents —Antibodies to ACSS1 and ACSS2 were purchased from Proteintech (Cat. 171138-1-AP) and Cell Signaling (Cat. 3658), respectively. Rotenone and oligomycin A were purchased from Cayman Chemical Company, glyceryl triacetate (GTA) was purchased from ACROS Organics, and all other chemical compounds were purchased from Sigma. Rotenone and oligomycin A were reconstituted in DMSO and added to the cells at respective concentrations of 1 μM and 1 μM. Aqueous solutions of GTA, GTP, and GTB were added to the cells at final concentrations of 0.25% *v*/*v*.

Starvation-coupled Viability and ATP Assays—Cells were seeded at density of 8×10^3 cells per well of a 96-well plate (Greiner) in triplicates per condition in the RPMI 1640 medium (Biological Industries) and supplemented with 10% FBS, 0.3 g/liter L-glutamine (HyClone) and 2 g/liter D-glucose (Sigma) 12–16 h prior to initiation of starvation. Medium was then exchanged to basal RPMI 1640 medium containing defined supplements, metabolites, and/or pharmacologically active compounds for 30–36 h. As a source of acetate, 0.25% GTA was added to the defined medium. In the cases of sodium acetate and glycerol, to obtain equivalent amounts of of GTA, 35 mM sodium acetate (pH 7.0) and 12 mM glycerol was added to the conditioned medium. Viability was assayed using resazurin reagent (Biotium) in accordance with manufacturer's protocol. ATP was measured after 24–30 h of incubation in defined medium using CellTiter-Glo luminescent reagent (Promega). Fluorescent and luminescent signals were read on Synergy H1 microplate reader (BioTek Instruments).

Cell Proliferation Assay—MEL697 cells were seeded into 24-well plates (Greiner) at density of 2×10^4 cells per well, in duplicates per condition, 12–16 h prior to experimentation. To measure cellular proliferation in defined medium, cells were grown in plain RPMI 1640 medium in the absence of FBS and supplemented with GTA, Gln, or both for 30 h. At this point, every 2 h cells from duplicate wells were gently scraped into the medium and counted using Countess Automated Cell Counter (Invitrogen).

Crystal Violet Staining—MEL697 cells were seeded into 96 well plates at density of 8×10^3 cells per well in triplicates per condition in complete RPMI 1640 medium 12–16 h prior to experimentation. Medium was then exchanged to either the complete medium, or the defined RPMI 1640 medium supplemented with 0, 1, 5, or 10% FBS in the absence or presence of 0.3 g/L L-glutamine, 0.25% GTA, or both for 48 h. Viability was assessed by resazurin, subsequently cells were washed with PBS, fixed in 4% formaldehyde for 10 min, and the adherent cells were stained with 0.5% Crystal Violet.

shRNA-mediated Gene Silencing—TRC lentiviral shRNA vectors were obtained from Sigma. The ACSS1 was targeted by clone TRCN0000045380 and ACSS2 with combination of TRCN0000045563, TRCN0000045565, TRCN0000045566, and TRCN0000045567. The control shRNA is the pLKO.1-TRC control (Addgene, plasmid 10879). Production of viral particles and transduction of target cells was conducted as described elsewhere. Gene expression changes were assessed by RT-qPCR as we previously reported (23), using the following primer sequences: ACSS1 forward, GTGCAGAGTCCTTGGCTGGG, ACSS1 reverse, TTCTTCAGCTCCACCACGCG, ACSS2 forward, CGAGGCCCTGCAGAAGTGTC, and ACSS2 reverse, GAGTCACCCATGCCGAGCTC.

Animal Studies—NOD/scid/IL2Rgnull (NSG) mice were bred at IU Simon Cancer Center In-Vivo Therapeutic Core facility. 8-week-old female animals were subcutaneously implanted with 1 million MEL526 cells that were lentivirally transduced to express shRNA hairpins against control, ACSS1, or ACSS2, in 100 μl serum free medium into the right hind flank. Xenograft size was measured three times a week with a digital caliper and the ellipsoidal tumor volumes were recorded. All procedures were conducted in accordance with the principles outlined in the NIH Guide for the Care and Use of Laboratory Animals and were approved by the Indiana University Institutional Animal Care and Use Committee (IACUC).

Cellular Respirometry—Oxygen consumption rate (OCR) of cultured cells was measured with an XF24 extracellular flux analyzer (Seahorse Bioscience). Cells were seeded at 5×10^4 cells per well. One day before the experiment cell culture medium was exchanged for freshly prepared RPMI 1640 medium supplemented either with 2 g/liter D-glucose, 0.25% GTA, or 0.3 g/liter L-glutamine, and 2% serum. After 16-h treatment course, measurements were performed at 37 °C in a bath solution of fresh RMPI medium supplemented as above. Following three baseline OCR measurements, wells were sequentially injected with 1 μM oligomycin A, 60 μM 2,4-dinitrophenol (DNP), and 1 μM rotenone + 1 μM antimycin A. Once injected, each compound was present in the bath medium for the duration of the experiment. Three OCR measurements were performed after each injection. To ensure that the culture maintained sufficient oxygenation, a 3-min mix, 2-min wait cycle occurred prior to each 3-min measurement.

Statistical Analyses—Unless stated otherwise, data presented are mean ± S.D. in triplicates per condition ($n = 3$). Statistical analyses were done using GraphPad Prism 5, with statistical significance determined by Holm-Sidak method.

Results

Acetate Supplementation Sustains Mutant BRAF Melanoma Cell Viability, and Proliferation in Glucose-deprived Cells—To gain insight into novel glucose-independent metabolic path-

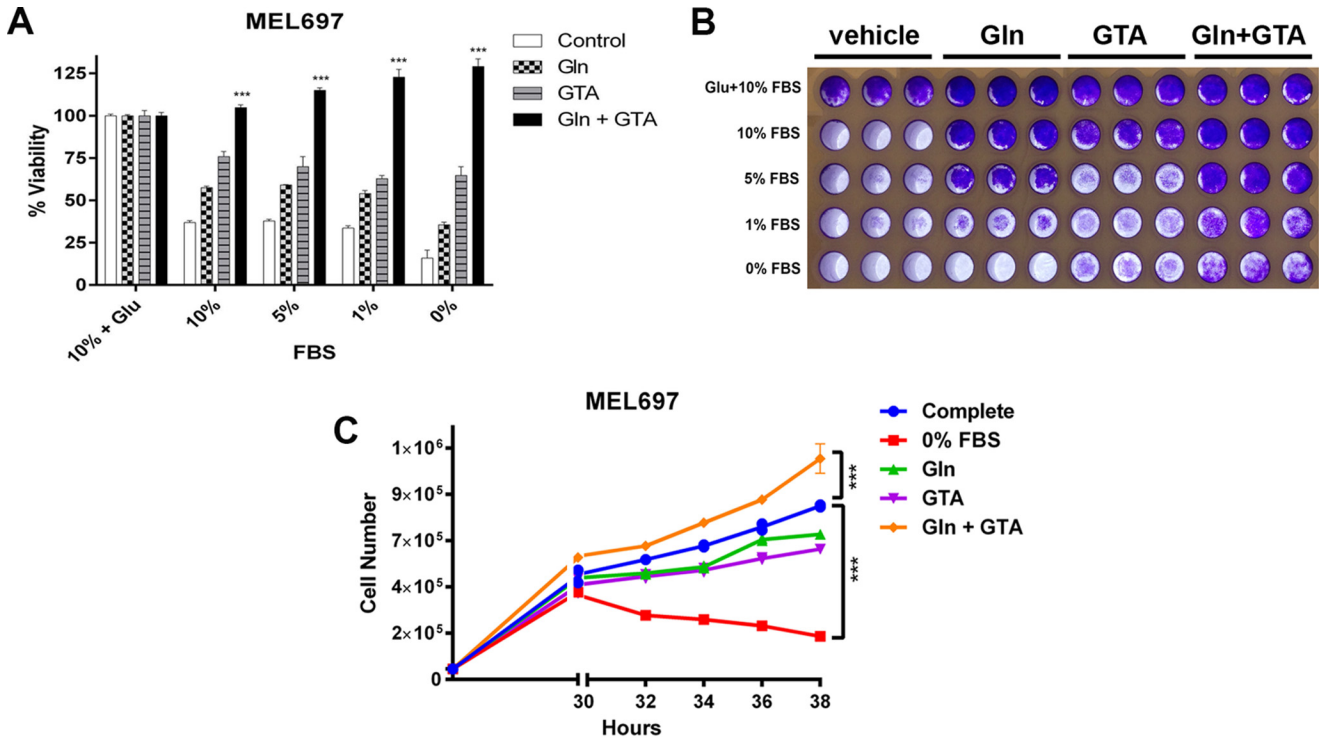

FIGURE 1. **Acetate supplementation restores cell viability and proliferation in glucose-deprived MEL697 melanoma cells.** *A*, cell viability of MEL697 cells grown in defined medium with added nutrients as indicated. Viability was assessed using a modified Alamar Blue reagent by fluorometry. Values represent averages of triplicates. Statistical analysis was conducted using Bonferroni's Multiple Comparison Test; ***, $p < 0.001$. *B*, crystal violet staining of MEL697 cells cultured in a basal RPMI medium supplemented with indicated nutrients. *Glu*, glucose; *Gln*, glutamine. *C*, proliferation of MEL697 cells grown in basal RPMI medium supplemented with nutrients as indicated; ***, $p < 0.001$.

ways that may support melanoma cell survival, we developed a starvation assay using RPMI medium lacking glucose and glutamine (defined medium), and by gradual reduction of serum concentrations to 0%. MEL697 melanoma cells harboring the $BRAF^{V600E}$ mutation are rapidly dividing cells that require constant supply of carbon (glucose) and nitrogen (glutamine) sources to support cell survival and proliferation. We exploited these features of MEL697 cells to develop glucose and serum starvation assay to study glucose-independent metabolic pathways. MEL697 were seeded in regular culture medium in a 96-well plate for 12–16 h. This regular medium was then replaced with defined medium containing glucose plus 10% serum or without glucose plus decreasing concentrations of serum from 10 to 0%. To this medium, glutamine (Gln) or GTA, or Gln plus GTA, was added as indicated (Fig. 1*A*). GTA, also known as triacetin has been used as a source of acetate for cancer cells, mice, and to treat infants with Canavan disease (24, 25). To quantify glucose-independent acetate metabolism, we adopted an Almar Blue-based cell viability assay. The results indicated that in glucose-deprived cells, acetate or glutamine alone was not sufficient to maintain cell viability, whereas the combination of acetate and glutamine significantly restored the viability of melanoma cells (Fig. 1*A*). Subsequent to cell viability determinations, cells were subjected to formaldehyde fixation and stained with crystal violet to visualize the intact cells that adhered to the plate. Although cells exposed to 10% serum with glucose were stained with crystal violet, there was no staining of cells observed in the absence of glucose. Glutamine, even in the absence of glucose retained crystal violet staining in cells cultured up to 5% serum. GTA supplementation maintained crystal violet staining of cells in 10% serum even in the absence of glucose. Remarkably, consistent with the results of cell viability assays, cells cultured in GTA- and Gln-containing medium were positive for crystal violet stain even in the absence of serum and glucose (Fig. 1*B*). Since acetate supplementation cooperated with glutamine in restoring viability of cells in the absence of glucose, we asked if the combination of acetate and glutamine could support cell proliferation. MEL697 cells were plated in defined medium as indicated in Fig. 1, and 30 h postincubation in the defined medium, cell number counting revealed that the combination of acetate (GTA) and glutamine was sufficient to support cell proliferation even in the absence of glucose and serum (Fig. 1*C*). Cells incubated in the medium without serum, glutamine and glucose maintained cell growth using the nutrients that were left on the plate from the original medium in which cells were seeded. However, after 30 h of incubation in medium without serum, glutamine, and glucose led to steady decrease in cell number compared with cells incubated in complete medium ($p < 0.001$). Remarkably, even in the absence of glucose and serum, cells incubated in glutamine plus GTA sustained cell proliferation that was significantly higher than that of the cell growth in complete medium ($p < 0.001$). Percent change in cell number was also plotted (supplemental Fig. S1).

Glutamine but Not Acetate Supports the Viability of Mutant NRAS and Wild-type BRAF/NRAS Melanoma Cells Deprived of Glucose—Although BRAF mutation is observed in 50% of melanomas, nearly 20% of melanomas harbor mutations in NRAS

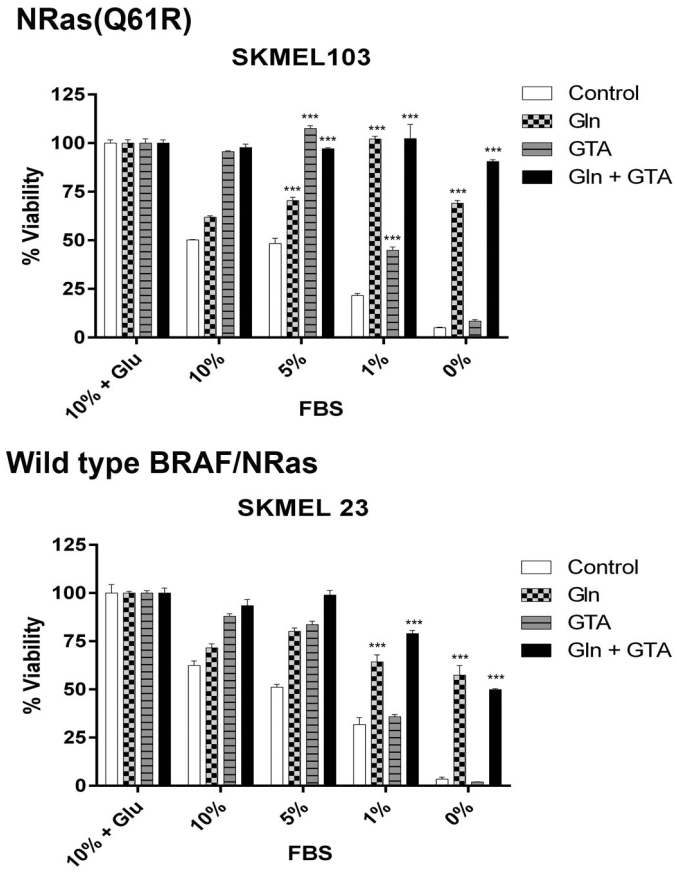

FIGURE 2. **Glutamine but not acetate reverses the effects of glucose starvation in a subset of melanoma.** MEL103 ($NRas^{Q61R}$) and SKMEL23 (BRAF/NRas-wild-type) melanoma cells were subjected to glucose-starvation assay in the presence of acetate or glutamine or in combination and cell viability was assessed. ***, $p < 0.001$.

and also there are cases where these genes are not mutated (26). To test whether acetate has similar effects in NRAS-mutant and BRAF/NRAS-wild-type cells, MEL103 ($NRAS^{Q61R}$) and SKMEL23 (BRAF/NRAS wild-type) melanoma cells were subjected to the same starvation assay as described above. Glutamine supplementation was sufficient to restore viability in both MEL103 and SKMEL23 cells lines, and GTA supplementation did not improve the cell viability (Fig. 2). Consistent with the cell viability data, cell number counting in a short-term culture in the absence of glucose revealed that glutamine was sufficient to support proliferation of MEL103 and SKMEL23 cells (supplemental Fig. S2).

Acetate Dependence in BRAF-mutant Melanoma Cells—Having demonstrated that acetate could replace glucose as a carbon source in mutant BRAF but not in NRAS mutant or BRAF/NRAS-wild-type melanoma cells, we extended these observations to commonly used melanoma cell lines. A375 and MEL526 are BRAF mutant melanoma cells that are widely used to study melanoma biology (27, 28). A375 and MEL526 were subjected to the defined medium as described above and cell viability was assessed. The results showed that glutamine supplementation was not sufficient to restore the viability but when combined with acetate, cell viability was restored significantly under glucose deprivation (Fig. 3*A*). To further substantiate these results, we measured ATP levels by luminescence-based assay. A375 and MEL526 cells were subjected to starvation conditions as described above and total ATP levels determined. GTA and glutamine together significantly restored ATP levels in the absence of glucose, recapitulating results of the cell viability data (Fig. 3*B*).

Melanoma Cells Metabolize Acetate, but Not Propionate or Butyrate—Short chain fatty acid oxidation fuels energy production in cells. Acetate, propionate, and butyrate are two, three, and four carbon short chain fatty acids, respectively (Fig. 4*A*). GTA, glyceryl tripropionate (GTP), and glyceryl tributyrate (GTB) are metabolized by normal and tumor cells (25, 29, 30). To test whether melanoma cells can utilize other short-chain fatty acids, or if the proliferative effects are limited to acetate, we performed cell viability assay for MEL526 and A375 cells in the presence of either GTA, GTP, or GTB in combination with glutamine. The observed effects of metabolic mediations that could support cell viability in the absence of glucose were limited to acetate (Fig. 4*B*). Because GTA metabolism can yield acetate and glycerol, to confirm the observed effects are due to acetate but not glycerol, we conducted cell viability assay in the presence of sodium acetate or glycerol. MEL526 and A375 cells were subjected to conditioned medium in the presence of acetate or glycerol. Similar to the effects of GTA, sodium acetate but not glycerol restored viability of cells in the absence of serum and glucose (supplemental Fig. S3) ($p < 0.001$).

Glucose-independent Acetate Metabolism in Melanoma Involves Oxidative Phosphorylation—Our previous report (23), and studies by others (31, 32), suggest that melanoma cells are highly dependent on glycolysis. This led us to hypothesize that glucose-deprivation imposes oxidative phosphorylation (OXPHOS)-dependent acetate metabolism in melanoma cells. To test this, A375 and MEL526 cells were cultured in defined medium containing 10% serum with (pink bars) or without glucose (gray bars) in the presence of either glutamine, GTA, or a combination of both, and treated with OXPHOS inhibitors oligomycin A or rotenone (Fig. 5*A*). Although neither oligomycin A nor rotenone exposure was cytotoxic to melanoma cells in the presence of glucose, viability of A375 and MEL526 cells was dramatically decreased by these OXPHOS inhibitors in the absence of glucose. To further confirm these results, A375 cells were cultured in the defined medium with or without glucose and in the presence or absence of glutamine plus GTA, and oxygen consumption rate (OCR) and extracellular acidification rate (ECAR) were measured. A dramatic increase in basal OCR was recorded in the absence of glucose (Fig. 5*B*). However, a reduced ECAR was recorded in cells cultured in glucose-deplete medium (Fig. 5*C*). These results suggest a metabolic shift from glycolysis to OXPHOS. Although DNP induced OCR in the presence of glucose, in the absence of glucose, GTA plus glutamine failed to show DNP response. The following two reasons may explain this failure to stimulate OCR by DNP. As shown in Fig. 5*A*, OXPHOS inhibitors are cytotoxic to melanoma cells in the absence of glucose and therefore DNP failed to stimulate OCR after oligomycin injection. A mechanistic explanation to this DNP response is that acetate to acetyl-CoA conversion requires ATP (18). Since oligomycin A inhibits ATP production, cells are unable to metabolize acetate in glucose-deplete medium and hence due to substrate limitations, DNP

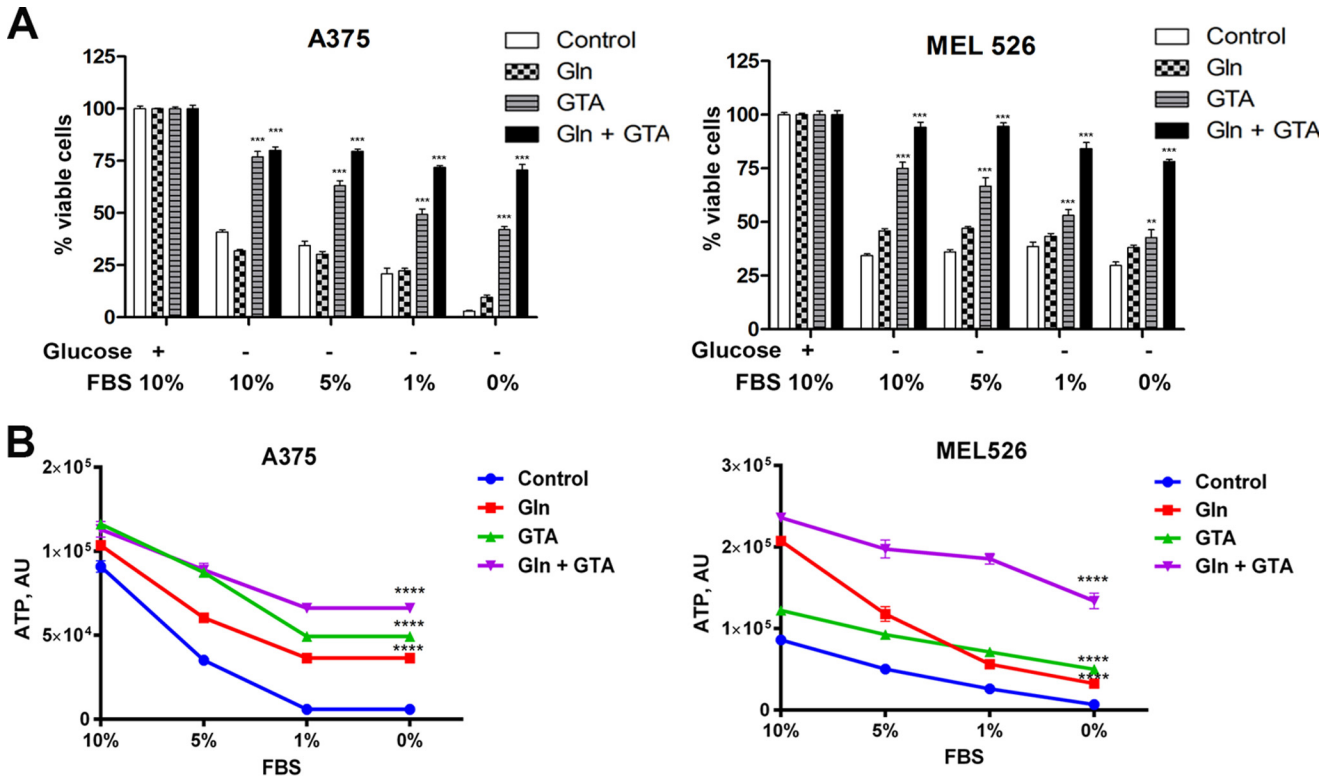

FIGURE 3. **Acetate dependence in BRAF mutant melanoma.** *A*, cell viability of A375 and MEL526 cells grown in defined medium with added nutrients as indicated. Viability was assessed using a modified Alamar Blue reagent by fluorometry. Values represent averages of triplicates. Statistical analysis was conducted using Bonferroni's Multiple Comparison Test; ***, $p < 0.001$. *B*, A375 and MEL526 cells cultured in defined medium and ATP levels assessed by luminescence-based assay; ***, $p < 0.001$.

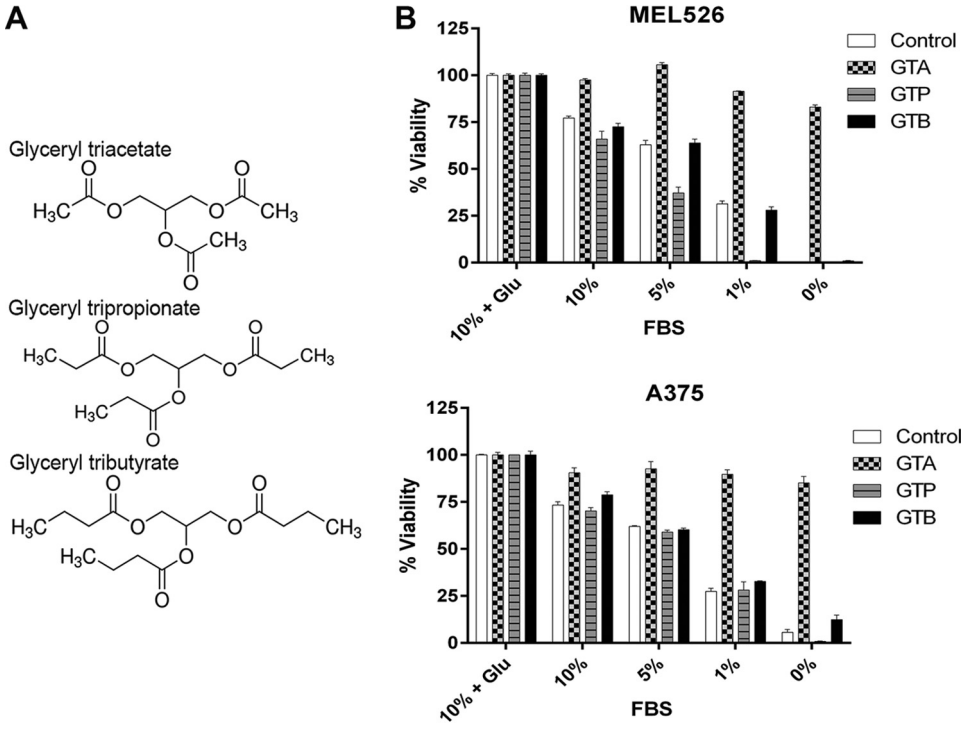

FIGURE 4. **Acetate but not propionate or butyrate supports glucose-independent cell viability.** *A*, structures of two, three, and four carbon sources as GTA, GTP, and GTB, respectively. *B*, cell viability of A375 and MEL526 cells in basal RPMI medium supplemented either with GTA or related short-chain fatty acids. Statistical analysis was conducted using Bonferroni's Multiple Comparison Test; ***, $p < 0.001$.

failed to stimulate OCR. The overall weaker response to DNP in melanoma cells is consistent with the findings that pyruvate transport into mitochondria is impaired in tumor cells (33–36). These observations led us to test whether mitochondria-permeable methyl-pyruvate allow DNP-mediated stimulation of OCR in melanoma cells. Although methyl-pyruvate produced a

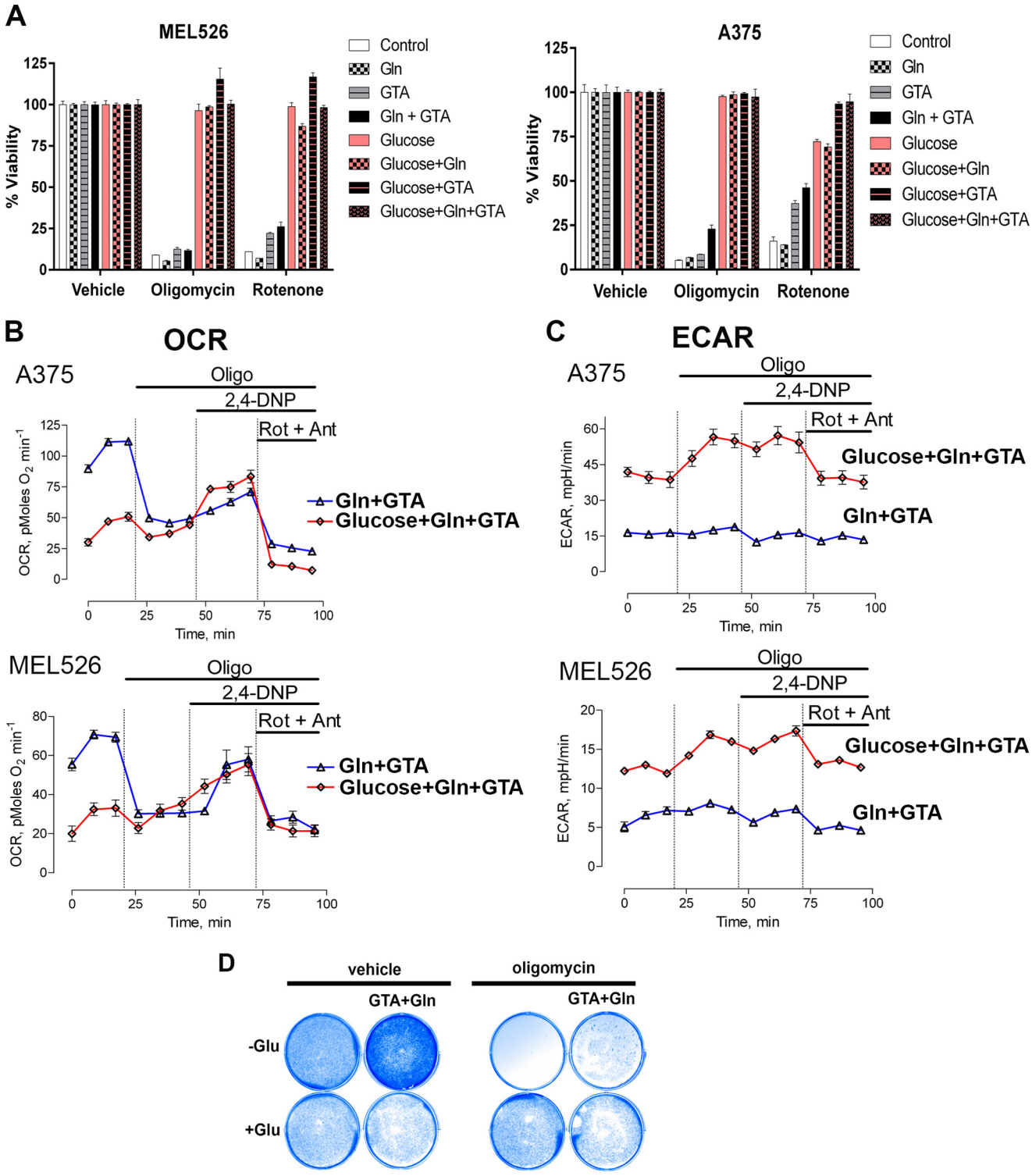

FIGURE 5. **Glucose-deprived cells switch to oxidative phosphorylation in acetate-mediated cell survival.** *A*, MEL526 and A375 cells were grown in a basal RPMI medium with indicated nutrients, in the presence of ATP synthase inhibitor oligomycin A or the electron transport chain complex I inhibitor rotenone and cell viability was assessed. *B*, oxygen consumption rate measurements of A375 and MEL526 cells in basal RPMI medium supplemented as indicated. Each data point is an average of five replicates. *C*, extra cellular acidification rate measurements of A375 and MEL526 cells in basal RPMI medium supplemented as indicated. *D*, crystal violet stain of A375 cells cultured in the presence or absence of glucose and/or GTA and glutamine and treated with either vehicle (DMSO) or oligomycin A.

robust induction of OCR by DNP in the presence of glucose, DNP failed to stimulate OCR in glucose-deplete condition (supplemental Fig. S4). To assess cytochrome *c* oxidase (COX) activity, mitochondria isolated from glucose-replete and glucose-deplete cells were subjected to COX assay. A significantly elevated COX activity was recorded in glucose-deplete cells compared with mitochondria from glucose-replete cells (supplemental Fig. S5). These results establish that mitochondrial substrate limitations

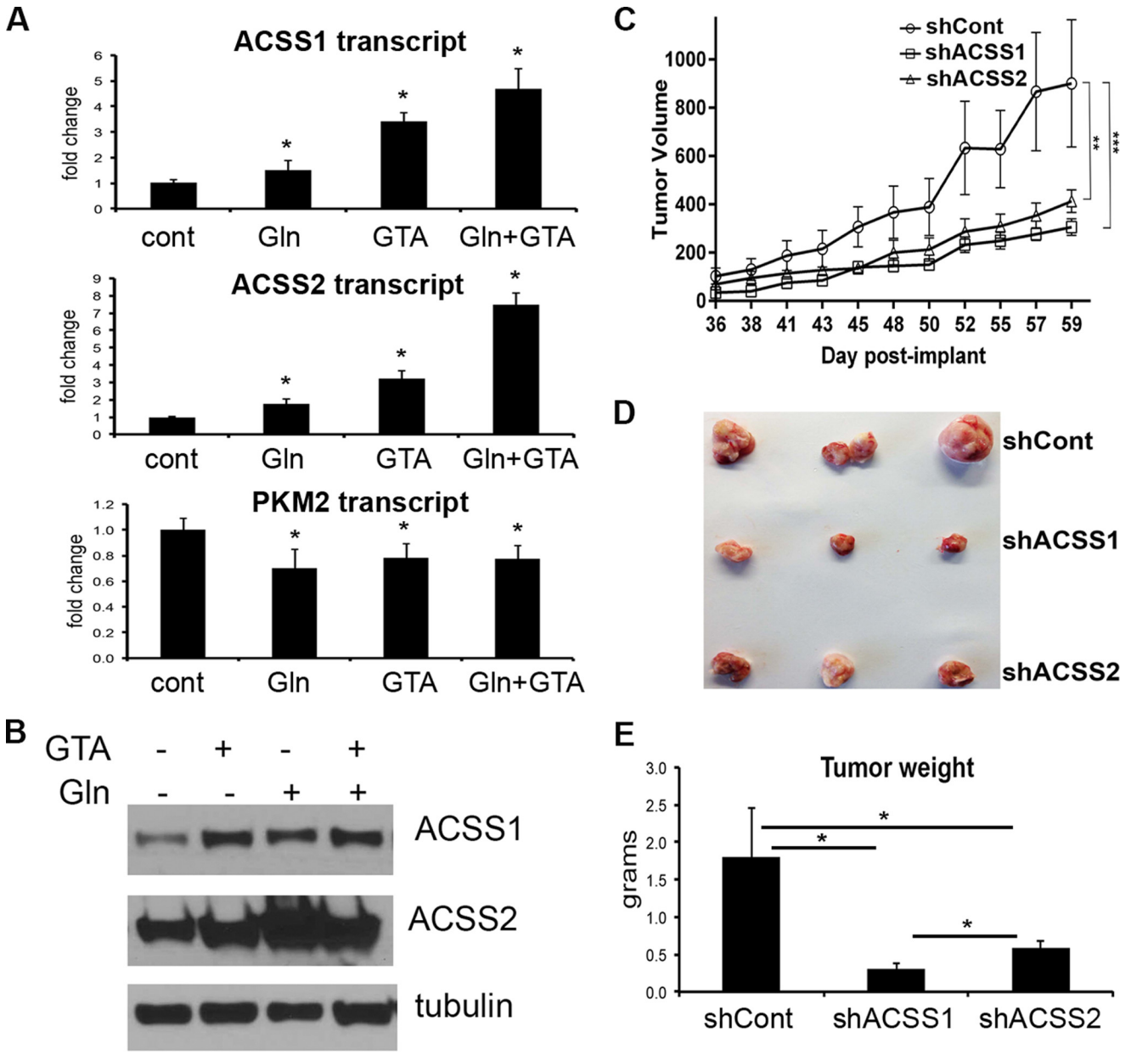

FIGURE 6. **Acetate supplementation induces ACSS1 and ACSS2 gene transcripts and depletion of these transcripts reduces the growth of melanoma xenografts.** *A*, quantitative transcript analysis of ACSS1, ACSS2, and PKM2. A375 cells were cultured in glucose-deprived medium supplemented with glutamine, or GTA, or in combination and the levels of indicated transcripts were assessed by quantitative real-time PCR. *B*, cell extracts prepared from conditions as in Fig. 6*A* were blotted with indicated antibodies. *C*, knockdown of ACSS1 or ACSS2 reduced melanoma xenograft tumor volumes, as assessed by ellipsoid tumor volume measurements. MEL526 cells were transduced with lentivirus expressing shCont, shACSS1, or shACSS2 and implanted in NSG mice. The average ± S.D. ($n = 3$) from each group at each time point is shown. **, $p < 0.01$; ***, $p < 0.001$. *D*, representative images of gross isolated tumor specimens. *E*, average tumor mass is plotted. *, $p < 0.01$ as compared with control.

stem DNP response in melanoma cells. To further substantiate these results, A375 cells were cultured in the presence or absence of glucose as well as glutamine plus GTA, and treated with oligomycin. Cells were fixed and stained with crystal violet to visualize intact adherent cells. Although glucose-replete cells stained with crystal violet, no staining was observed in glucose-starved A375 cells, suggesting that oligomycin was cytotoxic to cells in the absence of glucose (Fig. 5*C*).

Acetate Metabolism Promotes Melanoma Tumor Growth in Mice—Having demonstrated that glucose-deprived melanoma cells switch to OXPHOS and metabolize acetate to maintain ATP levels and cell survival, we hypothesized that acetate supplementation promotes induction of ACSS1 and ACSS2 transcript levels. To test this, A375 cells cultured in glucose-deprived medium containing GTA or glutamine, or a combination of these nutrients, and transcript levels of ACSS1, ACSS2 and the glycolytic enzyme PKM2 were quantified. Although PKM2 transcript levels were not increased by acetate supplementation, transcript levels of ACSS1 and ACSS2 were increased by acetate supplementation, and were further enhanced when combined with glutamine (Fig. 6*A*). Consistent with the transcript levels, combined incubation of acetate plus glutamine increased the levels of ACSS1 and ACSS2 protein levels (Fig. 6*B*). These results led to the consideration that

depletion of ACSS1 or ACSS2 may reduce melanoma tumor growth in mice. To this end, MEL526 cells were transduced with lentivirus expressing shACSS1 or shACSS2 and the knockdown efficiency was assessed by RT-qPCR (supplemental Fig. S6). In agreement with the transcript data, depletion of ACSS1/2 reduced the levels of ACSS1/2 proteins (supplemental Fig. S6). ACSS1 knockdown reduced 80% of its transcript with no change in the levels of ACSS2 transcripts. ACSS2 knockdown depleted nearly 90% of its transcripts with a small increase in the levels of ACSS1 transcript. To assess the effects of ACSS1 and ACSS2 knockdown on melanoma tumor growth in mice, MEL526 cells were transduced with these lentiviral shRNAs and implanted in NSG mice subcutaneously, as we previously reported (23). Depletion of ACSS1 or ACSS2 significantly reduced the growth of tumors as compared with the control group (Fig. 6*C*). Tumors were collected from the mice and the mass of the tumors recorded. Consistent with the reduced tumor growth, depletion of ACSS1 or ACSS2 showed a significant reduction in tumor weight (Fig. 6, *D* and *E*). Collectively, *in vitro* and *in vivo* results presented here provide strong evidence for acetate-dependence in melanoma.

Discussion

Metabolic plasticity allows malignant cells to survive and proliferate in a nutrient-limited tumor microenvironment. Melanoma cells provide an excellent model system to study this metabolic plasticity, as the development of resistance to BRAF inhibitors involves a metabolic switch from glycolysis to OXPHOS (9–12). Our present study shows that glucose-deprived melanoma cells heavily rely on acetate metabolism for survival. Although recent studies have implicated nucleo-cytoplasmic acetate assimilating enzyme ACSS2 in tumor growth (20–22), we now show that melanoma tumor growth *in vivo* is also dependent on mitochondrial enzyme ACSS1.

Remarkably, our findings establish that acetate dependence is specific to mutant BRAF but not mutant NRAS or wild-type BRAF/NRAS melanoma cells. Although NRAS mutation promotes glutamine metabolism and supports the growth of pancreatic ductal adenocarcinoma (37), unique metabolic adaption mediated by mutant BRAF has remained unclear. Our results demonstrate that melanoma cells harboring BRAF mutation readily adapt to acetate as a carbon source in place of glucose. Since melanoma therapy targeting mutant BRAF leads to reduction in glycolysis and increase in mitochondrial functions (4, 9–12), it is possible that mitochondrial acetate metabolism may contribute to rapid development of resistance to this therapy. In addition, we demonstrated that NRAS mutant and BRAF/NARS-wild type melanoma cells primarily relay on glutamine but not acetate. These observations clearly establish a link between oncogenic mutations and specific metabolic adaptations.

Glucose-deprived melanoma cells are dependent on acetate to sustain ATP levels and cell proliferation in cooperation with glutamine metabolism, yet the sources of acetate *in vivo* remain unclear. However, a broad range of acetate concentration (50–200 μM) was detected in human and murine blood (38–40). Carbohydrate fermentation in human gut yields short chain fatty acids including acetate, propionic, and butyric acids, which contributes to high levels of acetate in the blood (39). Supplementation of melanoma cells with glycerol derivative of acetate but not propionate or butyrate was sufficient to restore cell viability from glucose deprivation. Since GTA stimulated induction of ACSS1 and ACSS2 transcripts in glucose-deprived cells, and GTP and GTB did not reverse the effects of glucose deprivation, GTA-derived acetate can be attributed to the biological, biochemical and metabolic results of our studies. Although advanced stage melanoma is highly metastatic, primary melanoma resides in the skin. The skin harbors a rich microbiome (41), and it is an open question as to whether the skin microbiome can be a source of acetate for a subset of melanoma. While this paper was under review, a series of reports showed that gut microbiome contributes to acetate-mediated metabolic syndrome (42–45). The reliance on aerobic glycolysis of melanoma cells increases lactate secretion, which reprograms the tumor microenvironment to evade the immune system and promote tumor growth (46). Since BRAF inhibitor-resistant melanoma showed reduced glucose uptake and glycolysis while retaining aggressive growth characteristics (9–12), it is tempting to speculate that these glucose-starved tumors may reprogram the microenvironment for the supply of acetate.

Results of cell viability from OXPHOS inhibitors-treated cells and OCR measurements from glucose-replete cells suggest that melanoma cells derive energy primarily from glycolysis. A metabolic adaptability was evident from the fact that OXPHOS inhibitors were not cytotoxic to melanoma cells in the presence of glucose. Conversely, glucose-starved cells showed a robust increase in basal OCR while maintaining low ECAR and were sensitive to OXPHOS inhibitors. The observation that in glucose-deplete cells, GTA plus glutamine failed to stimulate OCR by DNP is worthy of discussion. Importantly, acetate to acetyl-CoA conversion is an ATP-dependent process, which can be inhibited by oligomycin. However, oligomycin-resistant ATP from glycolysis can support mitochondrial acetate metabolism, which can supply NADH to electron transport chain and can respond to DNP. Because lack of glucose abrogates this response, it is reasonable to propose that mitochondrial acetate metabolism contributes to DNP response in the presence of glucose. Surprisingly, exposure to 0.55 mM DNP was not cytotoxic to melanoma cells and the DNP treatment caused an increase in ATP levels suggesting a metabolic adaptation to glycolysis (9). Several studies have shown that melanoma cells poorly respond to protonophore FCCP and are highly resistant to cytotoxic effects of OXPHOS inhibitors (47, 48). These observations are consistent with the findings that the development of resistance to BRAF inhibition was associated with gain of mitochondrial functions (9–12). Our results support a model in which mitochondrial acetate metabolism is critical to meet the cellular bioenergetics demands of melanoma cells. It is highly relevant to note that ACSS1 knock-out mice showed 50% reduction of ATP levels in skeletal muscle, and these mice were resistant to weight gain on a low carbohydrate, high-fat diet (49). Interestingly, genome analysis of thoroughbred horses revealed a positive selection for ACSS1 locus (50), and a polymorphism in ACSS1 was associated with elite racecourse performance of horses (51). These observations in the

context of our data may explain why melanoma is more commonly seen in horses than any other domesticated animals (52, 53). However, we show that depletion of ACSS1 or ACSS2 reduced the growth of melanoma xenografts. Although glucose starvation significantly decreases melanoma cell viability suggesting glucose as a primary metabolic choice, depletion of ACSS1 or ACSS2 caused a significant reduction in tumor growth *in vivo*. Based on these observations, it is reasonable to propose acetate metabolism as an Achilles' heel in mutant BRAF-driven melanoma. Since acetate to acetyl-CoA conversion is also an ATP-dependent reaction, we believe that the energy required for cytosolic acetate assimilation (ACSS2) is derived from mitochondrial acetate metabolism (ACSS1). In agreement with this notion, a recent study analyzing patient samples revealed that high levels of ACSS1 was associated with hepatocellular carcinoma tumor growth and malignancy (54). Collectively, these observations suggest that ACSS1 contributes to aggressive tumor growth.

Remarkably, glucose concentration is 3–10-fold lower in cancer cells than normal cells (55–57). Consistent with our observation that glucose starved melanoma cells readily adapt to acetate metabolism, lung cancer patients infused with labeled glucose revealed contributions of non-glucose nutrients to overall tumor metabolism (58). These observations suggest that tumor cells must rely on other sources of carbon to fill the carbon void created by glucose deficit. We propose that acetate metabolism in melanoma presents a potential targetable vulnerability. Importantly, ACSS1 and ACSS2 mutant mice develop normally without any overt phenotypes suggesting that ACSS1- and ACSS2-mediated acetate metabolism is dispensable for normal cell functions in mice (20, 49). Because resistance to BRAF inhibitor is associated with gain of mitochondrial functions (9–12), and that tumor cells devoid of mitochondrial DNA show delayed tumor growth (59), it is possible that concurrent targeting of ACSS1 and mutant BRAF may significantly improve clinical outcomes of treatment for patients with melanoma.

Author Contributions—S. R. N. conceived the project, designed the experiments and wrote the paper. A. J. L. performed majority of experiments and analyzed the data. J. H. performed OCR experiments. N. B., H. E. B., and R. L. K. analyzed the data.

Acknowledgments—We thank Navdeep Chandel for discussion. In vivo Therapeutics Core of IU Simon Cancer Center carried out mouse xenograft studies.

References

1. Vander Heiden, M. G., Cantley, L. C., and Thompson, C. B. (2009) Understanding the Warburg effect: the metabolic requirements of cell proliferation. *Science* **324,** 1029–1033
2. Semenza, G. L. (2013) HIF-1 mediates metabolic responses to intratumoral hypoxia and oncogenic mutations. *J. Clin. Invest.* **123,** 3664–3671
3. Bollag, G., Tsai, J., Zhang, J., Zhang, C., Ibrahim, P., Nolop, K., and Hirth, P. (2012) Vemurafenib: the first drug approved for BRAF-mutant cancer. *Nat Rev. Drug Discov.* **11,** 873–886
4. Parmenter, T. J., Kleinschmidt, M., Kinross, K. M., Bond, S. T., Li, J., Kaadige, M. R., Rao, A., Sheppard, K. E., Hugo, W., Pupo, G. M., Pearson, R. B., McGee, S. L., Long, G. V., Scolyer, R. A., Rizos, H., Lo, R. S., Cullinane, C., Ayer, D. E., Ribas, A., Johnstone, R. W., Hicks, R. J., and McArthur, G. A. (2014) Response of BRAF-mutant melanoma to BRAF inhibition is mediated by a network of transcriptional regulators of glycolysis. *Cancer Disc.* **4,** 423–433
5. Bollag, G., Hirth, P., Tsai, J., Zhang, J., Ibrahim, P. N., Cho, H., Spevak, W., Zhang, C., Zhang, Y., Habets, G., Burton, E. A., Wong, B., Tsang, G., West, B. L., Powell, B., Shellooe, R., Marimuthu, A., Nguyen, H., Zhang, K. Y., Artis, D. R., Schlessinger, J., Su, F., Higgins, B., Iyer, R., D'Andrea, K., Koehler, A., Stumm, M., Lin, P. S., Lee, R. J., Grippo, J., Puzanov, I., Kim, K. B., Ribas, A., McArthur, G. A., Sosman, J. A., Chapman, P. B., Flaherty, K. T., Xu, X., Nathanson, K. L., and Nolop, K. (2010) Clinical efficacy of a RAF inhibitor needs broad target blockade in BRAF-mutant melanoma. *Nature* **467,** 596–599
6. Wise, D. R., and Thompson, C. B. (2010) Glutamine addiction: a new therapeutic target in cancer. *Trends Biochem. Sci.* **35,** 427–433
7. Le, A., Lane, A. N., Hamaker, M., Bose, S., Gouw, A., Barbi, J., Tsukamoto, T., Rojas, C. J., Slusher, B. S., Zhang, H., Zimmerman, L. J., Liebler, D. C., Slebos, R. J., Lorkiewicz, P. K., Higashi, R. M., Fan, T. W., and Dang, C. V. (2012) Glucose-independent glutamine metabolism via TCA cycling for proliferation and survival in B cells. *Cell Metab.* **15,** 110–121
8. Hatzivassiliou, G., Zhao, F., Bauer, D. E., Andreadis, C., Shaw, A. N., Dhanak, D., Hingorani, S. R., Tuveson, D. A., and Thompson, C. B. (2005) ATP citrate lyase inhibition can suppress tumor cell growth. *Cancer Cell* **8,** 311–321
9. Haq, R., Shoag, J., Andreu-Perez, P., Yokoyama, S., Edelman, H., Rowe, G. C., Frederick, D. T., Hurley, A. D., Nellore, A., Kung, A. L., Wargo, J. A., Song, J. S., Fisher, D. E., Arany, Z., and Widlund, H. R. (2013) Oncogenic BRAF regulates oxidative metabolism via PGC1α and MITF. *Cancer Cell* **23,** 302–315
10. Roesch, A., Vultur, A., Bogeski, I., Wang, H., Zimmermann, K. M., Speicher, D., Körbel, C., Laschke, M. W., Gimotty, P. A., Philipp, S. E., Krause, E., Pätzold, S., Villanueva, J., Krepler, C., Fukunaga-Kalabis, M., Hoth, M., Bastian, B. C., Vogt, T., and Herlyn, M. (2013) Overcoming intrinsic multidrug resistance in melanoma by blocking the mitochondrial respiratory chain of slow-cycling JARID1B(high) cells. *Cancer Cell* **23,** 811–825
11. Vazquez, F., Lim, J. H., Chim, H., Bhalla, K., Girnun, G., Pierce, K., Clish, C. B., Granter, S. R., Widlund, H. R., Spiegelman, B. M., and Puigserver, P. (2013) PGC1alpha expression defines a subset of human melanoma tumors with increased mitochondrial capacity and resistance to oxidative stress. *Cancer Cell* **23,** 287–301
12. Pollak, M. (2013) Targeting oxidative phosphorylation: why, when, and how. *Cancer Cell* **23,** 263–264
13. Ward, P. S., and Thompson, C. B. (2012) Metabolic reprogramming: a cancer hallmark even warburg did not anticipate. *Cancer Cell* **21,** 297–308
14. Brogsitter, C., Zophel, K., and Kotzerke, J. (2013) 18F-Choline, 11C-choline and 11C-acetate PET/CT: comparative analysis for imaging prostate cancer patients. *Eur. J. Nucl. Med. Mol. Imag.* **40,** S18–27
15. Oyama, N., Akino, H., Kanamaru, H., Suzuki, Y., Muramoto, S., Yonekura, Y., Sadato, N., Yamamoto, K., and Okada, K. (2002) 11C-acetate PET imaging of prostate cancer. *J. Nucl. Med.* **43,** 181–186
16. Tsuchida, T., Takeuchi, H., Okazawa, H., Tsujikawa, T., and Fujibayashi, Y. (2008) Grading of brain glioma with 1–11C-acetate PET: comparison with 18F-FDG PET. *Nucl. Med. Biol.* **35,** 171–176
17. Yun, M., Bang, S. H., Kim, J. W., Park, J. Y., Kim, K. S., and Lee, J. D. (2009) The importance of acetyl coenzyme A synthetase for 11C-acetate uptake and cell survival in hepatocellular carcinoma. *J. Nucl. Med.* **50,** 1222–1228
18. Fujino, T., Kondo, J., Ishikawa, M., Morikawa, K., and Yamamoto, T. T. (2001) Acetyl-CoA synthetase 2, a mitochondrial matrix enzyme involved in the oxidation of acetate. *J. Biol. Chem.* **276,** 11420–11426
19. Yamamoto, J., Ikeda, Y., Iguchi, H., Fujino, T., Tanaka, T., Asaba, H., Iwasaki, S., Ioka, R. X., Kaneko, I. W., Magoori, K., Takahashi, S., Mori, T., Sakaue, H., Kodama, T., Yanagisawa, M., Yamamoto, T. T., Ito, S., and Sakai, J. (2004) A Kruppel-like factor KLF15 contributes fasting-induced transcriptional activation of mitochondrial acetyl-CoA synthetase gene AceCS2. *J. Biol. Chem.* **279,** 16954–16962
20. Comerford, S. A., Huang, Z., Du, X., Wang, Y., Cai, L., Witkiewicz, A. K., Walters, H., Tantawy, M. N., Fu, A., Manning, H. C., Horton, J. D., Ham-

mer, R. E., McKnight, S. L., and Tu, B. P. (2014) Acetate dependence of tumors. *Cell* **159,** 1591–1602
21. Mashimo, T., Pichumani, K., Vemireddy, V., Hatanpaa, K. J., Singh, D. K., Sirasanagandla, S., Nannepaga, S., Piccirillo, S. G., Kovacs, Z., Foong, C., Huang, Z., Barnett, S., Mickey, B. E., DeBerardinis, R. J., Tu, B. P., Maher, E. A., and Bachoo, R. M. (2014) Acetate is a bioenergetic substrate for human glioblastoma and brain metastases. *Cell* **159,** 1603–1614
22. Schug, Z. T., Peck, B., Jones, D. T., Zhang, Q., Grosskurth, S., Alam, I. S., Goodwin, L. M., Smethurst, E., Mason, S., Blyth, K., McGarry, L., James, D., Shanks, E., Kalna, G., Saunders, R. E., Jiang, M., Howell, M., Lassailly, F., Thin, M. Z., Spencer-Dene, B., Stamp, G., van den Broek, N. J., Mackay, G., Bulusu, V., Kamphorst, J. J., Tardito, S., Strachan, D., Harris, A. L., Aboagye, E. O., Critchlow, S. E., Wakelam, M. J., Schulze, A., and Gottlieb, E. (2015) Acetyl-CoA synthetase 2 promotes acetate utilization and maintains cancer cell growth under metabolic stress. *Cancer Cell* **27,** 57–71
23. Lakhter, A. J., Hamilton, J., Dagher, P. C., Mukkamala, S., Hato, T., Dong, X. C., Mayo, L. D., Harris, R. A., Shekhar, A., Ivan, M., Brustovetsky, N., and Naidu, S. R. (2014) Ferroxitosis: a cell death from modulation of oxidative phosphorylation and PKM2-dependent glycolysis in melanoma. *Oncotarget* **5,** 12694–12703
24. Segel, R., Anikster, Y., Zevin, S., Steinberg, A., Gahl, W. A., Fisher, D., Staretz-Chacham, O., Zimran, A., and Altarescu, G. (2011) A safety trial of high dose glyceryl triacetate for Canavan disease. *Mol. Genet. Metab.* **103,** 203–206
25. Tsen, A. R., Long, P. M., Driscoll, H. E., Davies, M. T., Teasdale, B. A., Penar, P. L., Pendlebury, W. W., Spees, J. L., Lawler, S. E., Viapiano, M. S., and Jaworski, D. M. (2014) Triacetin-based acetate supplementation as a chemotherapeutic adjuvant therapy in glioma. *Int. J. Cancer* **134,** 1300–1310
26. Fedorenko, I. V., Gibney, G. T., Sondak, V. K., and Smalley, K. S. (2015) Beyond BRAF: where next for melanoma therapy? *Br. J. Cancer* **112,** 217–226
27. Maragos, C. M., Wang, J. M., Hrabie, J. A., Oppenheim, J. J., and Keefer, L. K. (1993) Nitric oxide/nucleophile complexes inhibit the *in vitro* proliferation of A375 melanoma cells via nitric oxide release. *Cancer Res.* **53,** 564–568
28. Zakut, R., Topalian, S. L., Kawakami, Y., Mancini, M., Eliyahu, S., and Rosenberg, S. A. (1993) Differential expression of MAGE-1, -2, and -3 messenger RNA in transformed and normal human cell lines. *Cancer Res.* **53,** 5–8
29. Xu, M., Nagati, J. S., Xie, J., Li, J., Walters, H., Moon, Y. A., Gerard, R. D., Huang, C. L., Comerford, S. A., Hammer, R. E., Horton, J. D., Chen, R., and Garcia, J. A. (2014) An acetate switch regulates stress erythropoiesis. *Nat. Med.* **20,** 1018–1026
30. Cresci, G. A., Bush, K., and Nagy, L. E. (2014) Tributyrin supplementation protects mice from acute ethanol-induced gut injury. *Alcohol Clin. Exp. Res.* **38,** 1489–1501
31. Kaplon, J., Zheng, L., Meissl, K., Chaneton, B., Selivanov, V. A., Mackay, G., van der Burg, S. H., Verdegaal, E. M., Cascante, M., Shlomi, T., Gottlieb, E., and Peeper, D. S. (2013) A key role for mitochondrial gatekeeper pyruvate dehydrogenase in oncogene-induced senescence. *Nature* **498,** 109–112
32. Yun, J., Rago, C., Cheong, I., Pagliarini, R., Angenendt, P., Rajagopalan, H., Schmidt, K., Willson, J. K., Markowitz, S., Zhou, S., Diaz, L. A., Jr, Velculescu, V. E., Lengauer, C., Kinzler, K. W., Vogelstein, B., and Papadopoulos, N. (2009) Glucose deprivation contributes to the development of KRAS pathway mutations in tumor cells. *Science* **325,** 1555–1559
33. Olson, K. A., Schell, J. C., and Rutter, J. (2016) Pyruvate and Metabolic Flexibility: Illuminating a Path Toward Selective Cancer Therapies. *Trends Biochem. Sci.* **41,** 219–230
34. Schell, J. C., Olson, K. A., Jiang, L., Hawkins, A. J., Van Vranken, J. G., Xie, J., Egnatchik, R. A., Earl, E. G., DeBerardinis, R. J., and Rutter, J. (2014) A role for the mitochondrial pyruvate carrier as a repressor of the Warburg effect and colon cancer cell growth. *Mol. Cell* **56,** 400–413
35. Herzig, S., Raemy, E., Montessuit, S., Veuthey, J. L., Zamboni, N., Westermann, B., Kunji, E. R., and Martinou, J. C. (2012) Identification and functional expression of the mitochondrial pyruvate carrier. *Science* **337,** 93–96
36. Bricker, D. K., Taylor, E. B., Schell, J. C., Orsak, T., Boutron, A., Chen, Y. C., Cox, J. E., Cardon, C. M., Van Vranken, J. G., Dephoure, N., Redin, C., Boudina, S., Gygi, S. P., Brivet, M., Thummel, C. S., and Rutter, J. (2012) A mitochondrial pyruvate carrier required for pyruvate uptake in yeast, *Drosophila*, and humans. *Science* **337,** 96–100
37. Son, J., Lyssiotis, C. A., Ying, H., Wang, X., Hua, S., Ligorio, M., Perera, R. M., Ferrone, C. R., Mullarky, E., Shyh-Chang, N., Kang, Y., Fleming, J. B., Bardeesy, N., Asara, J. M., Haigis, M. C., DePinho, R. A., Cantley, L. C., and Kimmelman, A. C. (2013) Glutamine supports pancreatic cancer growth through a KRAS-regulated metabolic pathway. *Nature* **496,** 101–105
38. Nuutinen, H., Lindros, K., Hekali, P., and Salaspuro, M. (1985) Elevated blood acetate as indicator of fast ethanol elimination in chronic alcoholics. *Alcohol* **2,** 623–626
39. Pomare, E. W., Branch, W. J., and Cummings, J. H. (1985) Carbohydrate fermentation in the human colon and its relation to acetate concentrations in venous blood. *J. Clin. Invest.* **75,** 1448–1454
40. Richards, R. H., Dowling, J. A., Vreman, H. J., Feldman, C., and Weiner, M. W. (1976) Acetate levels in human plasma. *Proc. Clin. Dial. Transplant Forum* **6,** 73–79
41. Yu, Y., Champer, J., Beynet, D., Kim, J., and Friedman, A. J. (2015) The role of the cutaneous microbiome in skin cancer: lessons learned from the gut. *J. Drugs Dermatol.* **14,** 461–465
42. Zitak, M., Kovatcheva-Datchary, P., Markiewicz, L. H., Ståhlman, M., Kozak, L. P., and Bäckhed, F. (2016) Altered microbiota contributes to reduced diet-induced obesity upon cold exposure. *Cell Metab.* **23,** 1216–1223
43. Trajkovski, M., and Wollheim, C. B. (2016) Physiology: Microbial signals to the brain control weight. *Nature* **534,** 185–187
44. Reijnders, D., Goossens, G. H., Hermes, G. D., Neis, E. P., van der Beek, C. M., Most, J., Holst, J. J., Lenaerts, K., Kootte, R. S., Nieuwdorp, M., Groen, A. K., Olde Damink, S. W., Boekschoten, M. V., Smidt, H., Zoetendal, E. G., Dejong, C. H., and Blaak, E. E. (2016) Effects of gut microbiota manipulation by antibiotics on host metabolism in obese humans: A randomized double-blind placebo-controlled trial. *Cell Metab.* **24,** 63–74
45. Perry, R. J., Peng, L., Barry, N. A., Cline, G. W., Zhang, D., Cardone, R. L., Petersen, K. F., Kibbey, R. G., Goodman, A. L., and Shulman, G. I. (2016) Acetate mediates a microbiome-brain-beta-cell axis to promote metabolic syndrome. *Nature* **534,** 213–217
46. Colegio, O. R., Chu, N. Q., Szabo, A. L., Chu, T., Rhebergen, A. M., Jairam, V., Cyrus, N., Brokowski, C. E., Eisenbarth, S. C., Phillips, G. M., Cline, G. W., Phillips, A. J., and Medzhitov, R. (2014) Functional polarization of tumour-associated macrophages by tumour-derived lactic acid. *Nature* **513,** 559–563
47. Liang, X., De Vera, M. E., Buchser, W. J., Romo de Vivar Chavez, A., Loughran, P., Beer Stolz, D., Basse, P., Wang, T., Van Houten, B., Zeh, H. J., 3rd, and Lotze, M. T. (2012) Inhibiting systemic autophagy during interleukin 2 immunotherapy promotes long-term tumor regression. *Cancer Res.* **72,** 2791–2801
48. Kluza, J., Corazao-Rozas, P., Touil, Y., Jendoubi, M., Maire, C., Guerreschi, P., Jonneaux, A., Ballot, C., Balayssac, S., Valable, S., Corroyer-Dulmont, A., Bernaudin, M., Malet-Martino, M., de Lassalle, E. M., Maboudou, P., Formstecher, P., Polakowska, R., Mortier, L., and Marchetti, P. (2012) Inactivation of the HIF-1α/PDK3 signaling axis drives melanoma toward mitochondrial oxidative metabolism and potentiates the therapeutic activity of pro-oxidants. *Cancer Res.* **72,** 5035–5047
49. Sakakibara, I., Fujino, T., Ishii, M., Tanaka, T., Shimosawa, T., Miura, S., Zhang, W., Tokutake, Y., Yamamoto, J., Awano, M., Iwasaki, S., Motoike, T., Okamura, M., Inagaki, T., Kita, K., Ezaki, O., Naito, M., Kuwaki, T., Chohnan, S., Yamamoto, T. T., Hammer, R. E., Kodama, T., Yanagisawa, M., and Sakai, J. (2009) Fasting-induced hypothermia and reduced energy production in mice lacking acetyl-CoA synthetase 2. *Cell Metab.* **9,** 191–202
50. Gu, J., Orr, N., Park, S. D., Katz, L. M., Sulimova, G., MacHugh, D. E., and Hill, E. W. (2009) A genome scan for positive selection in thoroughbred horses. *PLoS ONE* **4,** e5767
51. Hill, E. W., Gu, J., McGivney, B. A., and MacHugh, D. E. (2010) Targets of selection in the Thoroughbred genome contain exercise-relevant gene SNPs associated with elite racecourse performance. *Anim. Genet.* **41,** 56–63

52. Miller, M. A., Moore, G. E., Bertin, F. R., and Kritchevsky, J. E. (2016) What's new in old horses? postmortem diagnoses in mature and aged equids. *Vet. Pathol.* **53,** 390–398
53. Phillips, J. C., and Lembcke, L. M. (2013) Equine melanocytic tumors. *Vet. Clin. North Am. Equine Pract.* **29,** 673–687
54. Björnson, E., Mukhopadhyay, B., Asplund, A., Pristovsek, N., Cinar, R., Romeo, S., Uhlen, M., Kunos, G., Nielsen, J., and Mardinoglu, A. (2015) Stratification of hepatocellular carcinoma patients based on acetate utilization. *Cell Rep.* **13,** 2014–2026
55. Hirayama, A., Kami, K., Sugimoto, M., Sugawara, M., Toki, N., Onozuka, H., Kinoshita, T., Saito, N., Ochiai, A., Tomita, M., Esumi, H., and Soga, T. (2009) Quantitative metabolome profiling of colon and stomach cancer microenvironment by capillary electrophoresis time-of-flight mass spectrometry. *Cancer Res.* **69,** 4918–4925
56. Birsoy, K., Possemato, R., Lorbeer, F. K., Bayraktar, E. C., Thiru, P., Yucel, B., Wang, T., Chen, W. W., Clish, C. B., and Sabatini, D. M. (2014) Metabolic determinants of cancer cell sensitivity to glucose limitation and biguanides. *Nature* **508,** 108–112
57. Balsa-Martinez, E., and Puigserver, P. (2015) Cancer cells hijack gluconeogenic enzymes to fuel cell growth. *Mol. Cell* **60,** 509–511
58. Hensley, C. T., Faubert, B., Yuan, Q., Lev-Cohain, N., Jin, E., Kim, J., Jiang, L., Ko, B., Skelton, R., Loudat, L., Wodzak, M., Klimko, C., McMillan, E., Butt, Y., Ni, M., Oliver, D., Torrealba, J., Malloy, C. R., Kernstine, K., Lenkinski, R. E., and DeBerardinis, R. J. (2016) Metabolic heterogeneity in human lung tumors. *Cell* **164,** 681–694
59. Tan, A. S., Baty, J. W., Dong, L. F., Bezawork-Geleta, A., Endaya, B., Goodwin, J., Bajzikova, M., Kovarova, J., Peterka, M., Yan, B., Pesdar, E. A., Sobol, M., Filimonenko, A., Stuart, S., Vondrusova, M., Kluckova, K., Sachaphibulkij, K., Rohlena, J., Hozak, P., Truksa, J., Eccles, D., Haupt, L. M., Griffiths, L. R., Neuzil, J., and Berridge, M. V. (2015) Mitochondrial genome acquisition restores respiratory function and tumorigenic potential of cancer cells without mitochondrial DNA. *Cell Metab.* **21,** 81–94